1. Supplementary Methods

A. Details on the experimental setup

Five $3'' \times 3''$ LaBr$_3$:Ce-detectors were positioned 22 cm away from a ^{137}Cs gamma-ray source, which resulted in an average full-energy efficiency of 1.50(5)% at an energy of 661.66 keV for the entire set-up. The ^{137}Cs had an average activity of 603(18) kBq. The lead shield had minimal thicknesses of 12.5 cm and 8.5 cm for the 72° and 144° groups, respectively. These thicknesses were chosen on the basis of a Monte-Carlo simulation with the program GEANT4 [17]. Data were recorded using a digitizer with 14 bit resolution and a sampling rate of 250 MHz (SIS3316 of Struck company). The gain of the detectors exhibited a temperature dependence of up to 10 keV. These gain shifts were corrected by repeating the energy calibration every ~35 min using the 661.66 keV transition of the ^{137}Cs source and a background line. The background caused by cosmic-rays and their decay products was a considerable challenge during the experiment. It was partly suppressed using five large plastic scintillators as veto detectors, which were positioned on top of the experimental set-up. The width of the time gate on the prompt coincidence peak (2.4 ns) was chosen to optimise the signal-to-random ratio and includes 90(3)% of $\gamma\gamma$-events. The values of δ given in the letter are corrected for the width of this time gate. The correction factor was determined in a separate measurement using a ^{60}Co source (which emits two coincident gamma-rays) considering the energy dependence of the time resolution.

B. Details on the QPM calculations

A calculation in the framework of the QPM has been performed in order to obtain additional insights in the $\gamma\gamma$-decay process. The QPM is a phenomenological, microscopic approach to nuclear structure. Its Hamiltonian is given by

$$H_{qpm} = H_{sp} + H_{pair} + H_m^{ph}. \tag{1}$$

H_{sp} is a one-body Hamiltonian (mean field). The Woods-Saxon potential with parameters from a global parametrisation is used for this term. All bound and quasi-bound single-particle states are accounted for, i.e. the QPM allows to investigate the properties of nuclei over a wide excitation energy range. H_{pair} accounts for monopole pairing with a constant, state independent, matrix element of the pairing force. It is fitted to odd-even mass differences of nuclei in the mass range of interest. The last term of supplementary Eq. (1) H_m^{ph} is a residual multipole interaction in the particle-hole channel which has a

separable Bohr-Mottelson form. The strength of the residual interaction is fixed through the properties of the neighbouring even-even nuclei, in particular through the excitation energy and $B(E2)$-strengths of the 2_1^+ states.

In the QPM procedure the Hamiltonian H_{qpm} is diagonalised stepwise. First, the BCS-equation based on $H_{sp} + H_{pair}$ are solved and the quasiparticle state formalism is implemented through the Bogoliubov transformation. Second, the phonon basis which describes 1p-1h excitations of an even-even core is built. It is obtained by solving the Quasiparticle Random-Phase Approximation (QRPA) equations. In the final step, the QPM Hamiltonian is diagonalised on the set of wave functions that, in present calculation for ^{137}Ba, contain a mixture of quasiparticle and different [quasiparticle $\otimes$ 1 phonon] configurations. Further details on the QPM are given in Ref. [16].

The calculations have been performed for the ground $I^\pi = 3/2^+$ and isomeric $I^\pi = 11/2^-$ states and also for the states with $I_n^\pi = 5/2^\pm$, $7/2^\pm$, $9/2^\pm$ as virtual intermediate states. Phonons with spin and parity from $1^\pm$ to $5^\pm$ and excitation energies up to 20 MeV have been used. The calculation yields about five thousand excited states for each I_n^π. The excitation energies and $B(SL)$ values of the lowest states in ^{137}Ba are presented in supplementary table 1 in comparison to experimental values. The calculation underestimates the energy of the $11/2_1^-$ level, while other quantities in supplementary table 1 are in reasonable agreement to data. The problem is traced back to the mean field in which the $2d3/2$ and $1h11/2$ orbitals are too close in energy. It may be solved by a small increase of the strength of the ls-term of the Woods-Saxon potential for the neutrons. We did not do this adjustment but instead used the experimental energies for the states in supplementary table 1 in calculation of α_{SLSL} coefficients. The running sums for $\alpha_{S'L'SL}$ are shown in figure 1. The dominating matrix elements are α_{E2M2}, α_{M1E3}. For the QPM results shown in the letter all stretched contributions, i.e. the ones shown in the top of figure 1 and listed on the left-hand side of supplementary table 2, were used. The non-stretched $J = 4$ $E2E3/E3E2$ and stretched $J = 5$ $E2E3/E3E2$ contributions were found to be negligible for the overall $\gamma\gamma$-decay branching ratio and for the angular correlation of the two emitted photons.

2. Supplementary Equations

A. Determination of the differential branching ratio δ

The quantity δ is defined as the differential $\gamma\gamma$-decay width $d^5\Gamma_{\gamma\gamma}/d\omega d\Omega d\Omega'$ integrated over the corresponding energy bin $\Delta E = E_h - E_l$, with $E_l < E_h \leq E_0/2$ (E_0 is the transition energy), and divided by the single-gamma decay width Γ_γ

$$\delta(E_l, E_h, \theta_{12}) := \frac{(4\pi)^2}{\Gamma_\gamma} \int_{E_l}^{E_h} d\omega \left. \frac{d^5\Gamma_{\gamma\gamma}}{d\omega d\Omega d\Omega'} \right|_{\theta_{12}}. \tag{2}$$

The integration must only be performed up to $E_0/2$ to take the Bose character of the photons into account and thus, to avoid double counting. θ_{12} is the average emission angle between the two gamma-rays, i.e. in our experiment $\theta_{12} = 72°$ and $144°$. Note that no integration over $d\Omega$ or $d\Omega'$ is performed, but rather the differential decay width is evaluated at the central angle θ_{12} between the two emitted gamma-rays. To motivate this definition it is instructive to look at δ, assuming a vanishing angular correlation of the two gamma-rays, i.e.

$$\frac{d^5\Gamma_{\gamma\gamma}^{\text{iso}}}{d\omega d\Omega d\Omega'} = \frac{1}{(4\pi)^2}\frac{d\Gamma_{\gamma\gamma}^{\text{iso}}}{d\omega} \tag{3a}$$

then

$$\delta^{\text{iso}}(E_l, E_h) = \frac{1}{\Gamma_\gamma}\int_{E_l}^{E_h}\frac{d\Gamma_{\gamma\gamma}^{\text{iso}}}{d\omega}d\omega \tag{3b}$$

and after integration over all gamma-ray energies (i.e. $E_l = 0$ and $E_h = E_0/2$)

$$\delta_{\text{tot}}^{\text{iso}} = \frac{\Gamma_{\gamma\gamma}^{\text{iso}}}{\Gamma_\gamma} . \tag{3c}$$

Thus δ corresponds just to the branching ratio in case of vanishing angular correlation.

Next we clarify, how δ is related to the experimentally observed intensities. Assuming N decays of the isomer have taken place, then

$$N'_{\gamma\gamma} = N \cdot \frac{1}{\Gamma}\int_{4\pi} d\Omega \int_{4\pi} d\Omega' \int_{E_l}^{E_h} d\omega \frac{d^5\Gamma_{\gamma\gamma}}{d\omega d\Omega d\Omega'}\epsilon_{\text{intr}}(\omega, \Omega)\epsilon_{\text{intr}}(E_0 - \omega, \Omega') \tag{4}$$

is the number of detected $\gamma\gamma$-events assuming an intrinsic detection efficiency of $\epsilon_{\text{intr}}(\omega, \Omega)$ for a gamma-ray of energy ω travelling in direction $\Omega = (\theta, \phi)$. The quantity Γ is the total decay width. The intrinsic efficiency ϵ_{intr} will only be non-vanishing if Ω overlaps with the solid angle covered by one of the detectors. Assuming that $d^5\Gamma_{\gamma\gamma}/d\omega d\Omega d\Omega'$ varies at most linearly over the angles subtended by a detector pair we obtain

$$N'_{\gamma\gamma} = N \cdot \frac{1}{\Gamma}\cdot(4\pi)^2\cdot\int d\omega \frac{d^5\Gamma_{\gamma\gamma}}{d\omega d\Omega d\Omega'}\Bigg|_{\theta_{12}}\left[\sum_{i<j}2\epsilon_{\text{abs}}^{(i)}(\omega)\epsilon_{\text{abs}}^{(j)}(E_0 - \omega)\right], \tag{5}$$

where i, j denotes the detector numbers $(1\ldots5)$ and $\epsilon_{\text{abs}}^{(i)}(\omega)$ is the absolute full-energy peak efficiency of detector i for gamma-rays emitted isotropically of energy ω. The term in brackets is the absolute efficiency for two gamma-ray detection, assuming *no* angular correlation

$$\epsilon_{\text{abs},\gamma\gamma}^{\text{iso}} := \sum_{i<j}2\epsilon_{\text{abs}}^{(i)}(\omega)\epsilon_{\text{abs}}^{(j)}(E_0 - \omega). \tag{6}$$

As explained below, this quantity can be determined rather well experimentally and is approximately independent from the gamma-ray energy ω. It is convenient to define the

quantity

$$N''_{\gamma\gamma}(\theta_{12}) = \frac{N'_{\gamma\gamma}(\theta_{12})}{\epsilon^{\text{iso}}_{\text{abs},\gamma\gamma}} \ . \tag{7}$$

This is the efficiency-corrected number of counts of $\gamma\gamma$-events in detector pair(s) with opening angle θ_{12}, under the assumption of *isotropic emission*. If the emission is isotropic, it follows immediately that $N''_{\gamma\gamma} = N_{\gamma\gamma} := N \cdot \Gamma_{\gamma\gamma}/\Gamma$. For the single-gamma decay a similar expression is obtained

$$N''_\gamma = \frac{N'_\gamma}{\epsilon^{\text{iso}}_{\text{abs},\gamma}}, \tag{8}$$

with

$$\epsilon^{\text{iso}}_{\text{abs},\gamma} = \sum_i \epsilon^{(i)}_{\text{abs}}(E_0). \tag{9}$$

Since the single-gamma decay is isotropic $N''_\gamma = N_\gamma := N \cdot \Gamma_\gamma/\Gamma$. Now we consider the ratio

$$\frac{N''_{\gamma\gamma}(\theta_{12})}{N''_\gamma} = \frac{N \cdot \frac{1}{\Gamma} \cdot (4\pi)^2 \cdot \int d\omega \frac{d^5\Gamma_{\gamma\gamma}}{d\omega d\Omega d\Omega'}|_{\theta_{12}}}{N \cdot \frac{\Gamma_\gamma}{\Gamma}} \tag{10}$$

and see that this corresponds exactly to the definition of δ in supplementary Eq. (2). Thus, experimentally the quantity δ from supplementary Eq. (2), is given by

$$\delta = \frac{N''_{\gamma\gamma}(\theta_{12})}{N''_\gamma} \ , \tag{11}$$

while $N''_{\gamma\gamma}$ and N''_γ are straight-forwardly determined from the experimentally measured number of counts $N'_{\gamma\gamma}$ and N'_γ by supplementary Eqs. (7) and (8). The measured counts of $\gamma\gamma$-events $N'_{\gamma\gamma}$ had to be further corrected for the missed events due to the small coincidence window of 2.4 ns. The used digitizer allowed to measure N'_γ and $N'_{\gamma\gamma}$ with a negligible dead time even at detector rates of several kHz. The efficiencies $\epsilon^{(i)}_{\text{abs}}(E_0)$ were determined before the actual experiment with a source measurement.

The product $\epsilon^{(i)}_{\text{abs}}(\omega)\epsilon^{(j)}_{\text{abs}}(E_0-\omega)$ depends on the energy of both gamma-rays. However, in the present experiment it was only possible to measure in an energy window defined by the condition $|E_1 - E_2| <350$ keV for background suppression. Inside this energy window, which corresponds to the energy range of 156 keV$< E_{1,2} < 506$ keV, the energy dependence of the full-energy efficiency $\epsilon^{(i)}_{\text{abs}}(\omega)$ can be approximated with the function $\epsilon^{(i)}_{\text{abs}}(\omega) = a_i \exp(-b\omega)$. Therefore the product $\epsilon^{(i)}_{\text{abs}}(\omega)\epsilon^{(j)}_{\text{abs}}(E_0 - \omega)$

$$\epsilon^{(i)}_{\text{abs}}(\omega)\epsilon^{(j)}_{\text{abs}}(E_0 - \omega) = a_i a_j \exp(-bE_0) \tag{12}$$

is approximately energy-independent. The energy dependence of $\epsilon^{(i)}_{\text{abs}}(\omega)$ was simulated with GEANT4 [17]. The simulated efficiencies were scaled to the measured efficiencies at an energy of 661.66 keV. Then for each detector i the parameters a_i and b were determined

through a fit of $\epsilon_{\text{abs}}^{(i)}(\omega) = a_i \exp(-b\omega)$ to the simulated and scaled efficiency curves in the energy window of interest. Thus, the $\gamma\gamma$-coincidence efficiency $\epsilon_{\text{abs}}^{(i)}(\omega)\epsilon_{\text{abs}}^{(j)}(E_0 - \omega)$ for each detector pair was determined.

In order to suppress the background it was necessary to impose the energy conditions $|E_1 - E_2| <300$ keV and $|E_1 - E_2| < 250$ keV for the 72° and 144°-groups, respectively. Thus, the values of $1.65(25) \cdot 10^{-6}$ and $0.63(19) \cdot 10^{-6}$ obtained for δ by evaluating supplementary Eq. (11) are only parts (86% and 80%) of the full values (which would require an energy gate of $|E_1 - E_2| <661.66$ keV). This restriction has been considered in the extraction of the total branching ratio $\Gamma_{\gamma\gamma}/\Gamma_\gamma$ included in Tab. 1.

The difference of the energy gates of the 72° and 144°-groups is due to the process we term 'sequential' Compton scattering. In this process the 661.66-keV gamma-ray of the single-gamma decay deposits a part of its energy in detector A ($E_A \approx 477$ keV) and is then scattered by $\sim 180°$ in the opposite direction. Next it scatters again on the ^{137}Cs source or the lead bricks by angles of $\sim 72°$ and $\sim 144°$ into detector B where it deposits the remaining part of its energy ($E_B \approx 125$ keV for 72° and $E_B \approx 172$ keV for 144°). The sum energy of both detectors $E_A + E_B$ is approximately ~ 603 and ~ 650 keV for the 72° and 144°-groups, respectively. Therefore the 'sequential' Compton scattering process does not prohibit the analysis of the $\gamma\gamma$-peak at 661.66 keV in case of the 72°-group due to the large energy difference of ~ 60 keV. On the other hand in case of the 144°-group the 'sequential' Compton scattering peak is only ~ 10 keV away from the $\gamma\gamma$-peak. Furthermore, the energy gate $|E_1 - E_2| < 300$ keV, which limits the accepted E_1 and E_2 values to the range from 181 to 481 keV, is not sufficient to suppress the 'sequential' Compton scattering process entirely. Hence we chose the energy gate $|E_1 - E_2| < 250$ keV, corresponding to a single gamma-ray energy range from 206 to 456 keV, for the 144°-group.

It is possible to increase the energy gate of the 72°-group to e.g. $|E_1 - E_2| < 400$ keV. However, this would increase the background close to the $\gamma\gamma$-peak in the sum energy spectra $E_1 + E_2$ drastically, since one of the two background gamma-rays has typically a low energy (< 180 keV). And, more importantly, the single energy spectra follow a $\omega^5 \cdot (E_0 - \omega)^5$ behaviour, neglecting the small octupole-dipole contribution, which can be seen Fig. 4a. Thus, the (single) energy spectra peak at $\omega = E_0/2$, which corresponds to $|E_1 - E_2| \sim 0$. Going away from the central energy $E_0/2$ reduces the signal rather quickly, while at the same time, the background increases, due to more copious low-energy gamma rays. Hence, a larger energy gate would degrade the signal-to-noise ratio.

B. Derivation of the equation for the differential $\gamma\gamma$-decay probability

Starting from Eqs. (A34a) and (A15) in Ref. [3] and following [18] one obtains after a few steps of angular momentum algebra supplementary Eq. (13) for the differential $\gamma\gamma$-decay width $d^5\Gamma_{\gamma\gamma}/(d\omega d\Omega d\Omega')$ for the transition from the first excited $I_i = 11/2^-$ state to the $I_f = 3/2^+$ ground state of ^{137}Ba. The equation is not only valid under the assumption that the angular momenta of the two emitted gamma-rays couple to $J = |I_i - I_f| = 4$ in a stretched way, i.e., that the sum of the multipolarities $L + L'$ of the two involved virtual transitions fulfills $L + L' = J = 4$, but also for non-stretched $E2E3$ and $E3E2$ transition and stretched $E2E3$ and $E3E2$ transitions with $J = 5$. Furthermore the selection rule $(-1)^{L'+S'+L+S} = \pi_i\pi_f = -1$ requires for the considered $11/2^- \rightarrow 3/2^+$ stretched $J = 4$ transition that one transition character is magnetic while the other one has to be electric. Non-stretched transitions of pure electric character are also possible, e.g. E2E3. S and S' denote the transition characters ($S = 0$ for electric and $S = 1$ for magnetic transition characters) and π_i, π_f denote the parities of the initial and final nuclear states. The expression for $d^5\Gamma_{\gamma\gamma}/(d\omega d\Omega d\Omega')$ is then given by

$$\frac{d^5\Gamma_{\gamma\gamma}}{d\omega d\Omega d\Omega'} = \frac{\omega\omega'}{96\pi^3} \sum_{\substack{JS_1'L_1'S_1L_1 \\ S_2'L_2'S_2L_2}} P_J'(S_1'L_1'S_1L_1)P_J'(S_2'L_2'S_2L_2) \sum_l a_l^{J\xi} P_l(\cos\theta_{12}) \tag{13}$$

where ξ stands for a full set of parameters $\{S_1'L_1'S_1L_1S_2'L_2'S_2L_2\}$ specifying the parities and angular momenta of the two emitted photons. The parameters a_J^ξ in front of the Legendre polynomials $P_i(\cos\theta_{12})$ are given in supplementary table 3. The functions $P_J'(S'L'SL)$ are the so-called generalised polarizabilities as given in Eq. (A19) in Ref. [3]

$$P_J'(S'L', SL, \omega'\omega) = (-1)^{S+S'}2\pi(-1)^{I_i+I_f}\omega^L\omega'^{L'}\cdot$$

$$\sqrt{2L+1}\sqrt{2L'+1}\sqrt{\frac{L+1}{L}}\sqrt{\frac{L'+1}{L'}}\frac{1}{(2L+1)!!(2L'+1)!!}\cdot$$

$$\sum_n \left[\begin{Bmatrix} L & L' & J \\ I_f & I_i & I_n \end{Bmatrix} \frac{\langle I_f||i^{L'-S'}M(S'L')||I_n\rangle\langle I_n||i^{L-S}M(SL)||I_i\rangle}{E_n - E_i + \omega} + \right.$$

$$\left. (-1)^{L+L'+J}\begin{Bmatrix} L' & L & J \\ I_f & I_i & I_n \end{Bmatrix} \frac{\langle I_f||i^{L-S}M(SL)||I_n\rangle\langle I_n||i^{L'-S'}M(S'L')||I_i\rangle}{E_n - E_i + \omega'} \right]\cdot \tag{14}$$

E_n and I_n are the excitation energies and the spins of the intermediate nuclear states through which the $\gamma\gamma$-decay proceeds. The definitions and conventions of the reduced matrix elements and the transition operators $M(SL)$ are the same as in Ref. [3]. It is convenient and interesting to separate P' into terms which involve intermediate states of a certain spin and parity I_n only. Thus it is possible to rewrite supplementary Eq. (14)

as

$$P'_{JI_n}(S'L', SL, \omega'\omega) = (-1)^{S+S'} 2\pi (-1)^{I_i + I_f} \omega^L \omega'^{L'} \cdot$$

$$\sqrt{2L+1}\sqrt{2L'+1}\sqrt{\frac{L+1}{L}}\sqrt{\frac{L'+1}{L'}}\frac{1}{(2L+1)!!(2L'+1)!!} \cdot$$

$$\left[\begin{Bmatrix} L & L' & J \\ I_f & I_i & I_n \end{Bmatrix} \alpha_{S'L'SL}(\omega) + (-1)^{L+L'+J} \begin{Bmatrix} L' & L & J \\ I_f & I_i & I_n \end{Bmatrix} \alpha_{SLS'L'}(\omega') \right], \tag{15}$$

with $P'_J = \sum_{I_n} P'_{JI_n}$ and

$$\alpha_{S'L'SL}(\omega) = \sum_n \frac{\langle I_f || i^{L'-S'} M(S'L') || I_n \rangle \langle I_n || i^{L-S} M(SL) || I_i \rangle}{E_n - E_i + \omega}. \tag{16}$$

Excluding the non-stretched $J = 4$ and all $J = 5$ contributions $d^5\Gamma_{\gamma\gamma}/(d\omega d\Omega d\Omega')$ in supplementary Eq. (13) depends on six $\alpha_{S'L'SL}(\omega)$ parameters: $\alpha_{M2E2}(\omega)$, $\alpha_{E2M2}(\omega)$, $\alpha_{M1E3}(\omega)$, $\alpha_{E3M1}(\omega)$, $\alpha_{M3E1}(\omega)$ and $\alpha_{E1M3}(\omega)$. For example in case of $\alpha_{E2M2}(\omega)$ the nucleus does a virtual $M2$-transition from the $11/2^-$ state to an intermediate $7/2^+$ state through which it decays via a virtual $E2$-transition to the ground state or for $\alpha_{M2E2}(\omega)$ a virtual $E2$-transition to an intermediate $7/2^-$ state through which it decays via a virtual $M2$-transition to the ground state. The corresponding sums run over all $7/2^+$ and $7/2^-$ states of the nucleus. Following Ref. [3] the denominator of supplementary Eq. (16) is approximated through $E_n - E_i + \omega \approx E_n - 0.5E_i$ to obtain approximate values for the $\alpha_{S'L'SL}(\omega)$ parameters that are independent of ω (ω is replaced by its average value $\omega = 0.5E_i$). This approximation is good in cases where $E_n - E_i \gg E_i$. Therefore with $(E_i = E_0)$

$$\alpha_{S'L'SL}(\omega) \approx \alpha_{S'L'SL} = \sum_n \frac{\langle I_f || i^{L'-S'} M(S'L') || I_n \rangle \langle I_n || i^{L-S} M(SL) || I_i \rangle}{E_n - 0.5E_0}. \tag{17}$$

It is desirable to extract all six parameters $\alpha_{S'L'SL}$ performing a fit based on supplementary Eq. (13) to the measured energy spectrum and angular correlations. However the statistics of the data and the number of data points does not allow to determine all six parameters. Therefore the free parameters were restricted to α_{E2M2} and α_{M1E3} that are expected to dominate the value of $\Gamma\gamma\gamma/\Gamma\gamma$ according to our calculation in the framework of the Quasiparticle-Phonon Model (QPM) (see supplementary table 2 and Fig. 1). In this calculation the value of $\Gamma\gamma\gamma/\Gamma\gamma$ considering α_{E2M2} and α_{M1E3} only, deviates by only $\sim 10\%$ from the full branching ratio $\Gamma\gamma\gamma/\Gamma\gamma$. The parameters $\alpha_{M2E2}(\omega)$, $\alpha_{E3M1}(\omega)$, $\alpha_{M3E1}(\omega)$ and $\alpha_{E1M3}(\omega)$ are expected from nuclear theory to have a minor influence on the branching ratio. In the following they were assumed to be zero. Then supplementary

equation (13) reduces then to Eq. (1) of the letter

$$\frac{d^5\Gamma_{\gamma\gamma}}{d\omega d\Omega d\Omega'} = A_{qq}(\alpha_{E2M2}^2, s) + \\ A_{od}(\alpha_{M1E3}^2, s) + A_x(\alpha_{E2M2} \cdot \alpha_{M1E3}, s), \tag{18}$$

with

$$A_{qq}(\alpha_{E2M2}^2, s) = \frac{\omega\omega'}{96\pi^3} \cdot \\ \left\{ \left(P_4'(E2M2, \omega'\omega)^2 + P_4'(M2E2, \omega'\omega)^2\right) \cdot \left(\frac{36}{25} + \frac{36}{245}P_2(\cos\theta_{12}) + \frac{16}{1225}P_4(\cos\theta_{12})\right) \right. \\ \left. + P_4'(E2M2, \omega'\omega)P_4'(M2E2, \omega'\omega) \cdot 2\left(\frac{12}{25}P_1(\cos\theta_{12}) + \frac{36}{175}P_3(\cos\theta_{12})\right) \right\},$$

$$A_{od}(\alpha_{M1E3}^2, s) = \frac{\omega\omega'}{96\pi^3} \cdot \\ \left\{ \left(P_4'(M1E3, \omega'\omega)^2 + P_4'(E3M1, \omega'\omega)^2\right) \cdot \left(\frac{12}{7} - \frac{3}{14}P_2(\cos\theta_{12})\right) \right. \\ \left. + \left(P_4'(M1E3, \omega'\omega)P_4'(E3M1, \omega'\omega)\right) \cdot 2\frac{9}{14}P_3(\cos\theta_{12}) \right\},$$

$$A_x(\alpha_{E2M2} \cdot \alpha_{M1E3}, s) = \frac{\omega\omega'}{(2I_i+1)\pi} \frac{2}{(4\pi)^2} \cdot \\ \left\{ \left(P_4'(E3M1, \omega'\omega)P_4'(E2M2, \omega'\omega) + P_4'(M1E3, \omega'\omega)P_4'(M2E2, \omega'\omega)\right) \cdot \right. \\ 2\sqrt{\frac{3}{5}}\left(\frac{72}{35}P_1(\cos\theta_{12}) - \frac{2}{35}P_3(\cos\theta_{12})\right) \\ + \left(P_4'(M1E3, \omega'\omega)P_4'(E2M2, \omega'\omega) + P_4'(E3M1, \omega'\omega)P_4'(M2E2, \omega'\omega)\right) \cdot \\ \left. 2\sqrt{\frac{3}{5}}\frac{6}{7}P_2(\cos\theta_{12}) \right\}. \tag{19}$$

Due to the assumption $\alpha_{M2E2}(\omega) = \alpha_{E3M1}(\omega) = \alpha_{M3E1}(\omega) = \alpha_{E1M3}(\omega) = 0$ each $P_J'(S'L', SL, \omega'\omega)$ in supplementary Eq.(19) has just one contributing α-parameter.

The two fit-parameters α_{E2M2} and α_{M1E3} were determined by a simultaneous fit of the data shown in Fig. 4a and the 144° data point from Fig. 4b. The 72° data point in Fig. 4b was not included, since it corresponds to the data in Fig. 4a, which were already included in the fit.

It should be remarked that the assumption $E_n - E_i \gg E_i$ for approximating ω through its average value $0.5E_0$ in supplementary Eq. (17) is not fully justified for the transition of interest for the states that are lowest in energy for a given spin quantum number I_n.

For example $E_i = 661.66$ keV and $E_n - E_i = 590$ keV for the lowest $7/2^+$ state of ^{137}Ba. The systematic errors that are introduced to the values given in Tab. 1 through this approximation are estimated to be of the order of $\sim 10\%$.

References

[17] Agostinelli, S. *et al.* GEANT4—a simulation toolkit. *Nucl. Instrum. Methods A* **506,** 250 (2003).

[18] Millener, D. J., Theory for 2-γ transitions: I, unpublished (2013), private communication.

| J^π | E_n (MeV) | | SL | $B(SL)$ (e^{2}fm^{2L}) | |
	exp.	calc.		exp.	calc.
$1/2^+$	0.283	0.176	E2	125	94
$11/2^-$	0.661	0.198	M4	$0.98\cdot10^3$	$1.11\cdot10^3$
$7/2^+$	1.251	1.432	E2	520	519
$5/2^+$	1.294	1.184	M1	$0.15\cdot10^{-2}$	$0.14\cdot10^{-2}$

Supplementary Table 1: Low lying states in ^{137}Ba and their decay transitions to the $3/2^+$ ground state as predicted by the QPM in comparison to data.
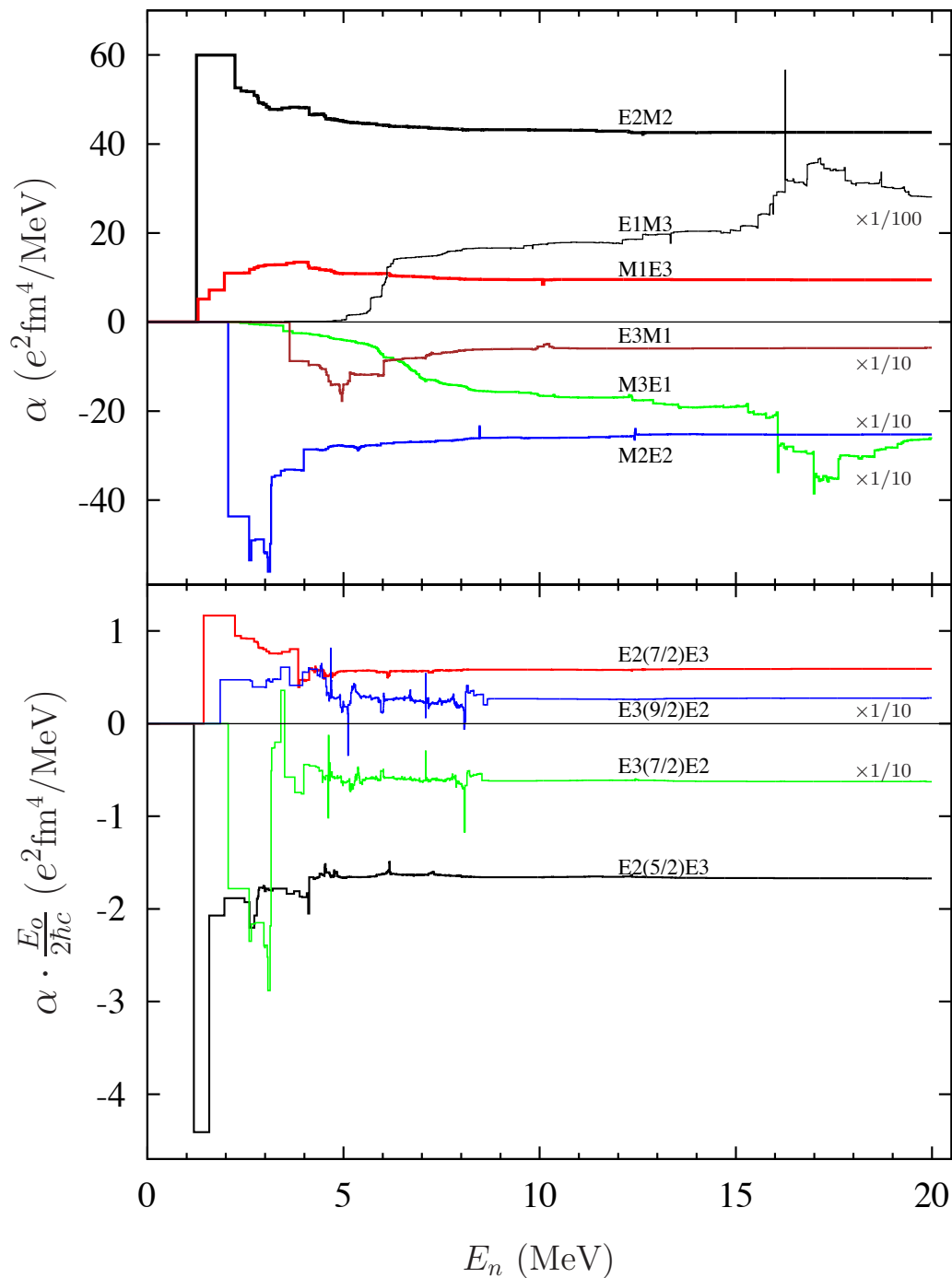
Supplementary Figure 1: Results of our QPM calculations: shown are the running sums of the various matrix elements $\alpha_{S'L'SL}$ defined in supplementary Eq. 17. The final values are the ones at 20 MeV, which are listed in supplementary table 2. Several contributions were to small to be visible un-scaled and the ordinate values should be multiplied by the given factors.

$J^\pi(|n\rangle)$	$S'L'$	SL	$\alpha_{S'L'SL}$ (e^2 fm^4/MeV)	$J^\pi(|n\rangle)$	$S'L'$	SL	$\alpha_{S'L'SL}$ (e^2 fm^5/MeV)
$9/2^+$	M3	E1	-2.63	$9/2^-$	E3	E2	16.54
$7/2^-$	M2	E2	-2.52	$7/2^-$	E3	E2	-37.49
$5/2^+$	M1	E3	9.47	$7/2^+$	E2	E3	353.35
$9/2^-$	E3	M1	-0.58	$5/2^+$	E2	E3	-997.46
$7/2^+$	E2	M2	42.60				
$5/2^-$	E1	M3	0.28				

Supplementary Table 2: Results of QPM calculations: final parameters $\alpha_{S'L'SL}$ as defined in supplementary Eq. 17. The $\gamma\gamma$-decay is mainly determined by α_{E2M2} and α_{M1E3}. The non-stretched (electric only) transitions, shown in the right-hand part, have very minor influence on the results and were not used.

J	$\xi = (S_1'L_1'S_1L_1)\cdot(S_2'L_2'S_2L_2)$	a_0^ξ	a_1^ξ	a_2^ξ	a_3^ξ	a_4^ξ	a_5^ξ
4	$M1E3^2$	$\frac{12}{7}$		$-\frac{3}{14}$			
4	$M1E3\cdot M2E2$		$\frac{144\sqrt{\frac{3}{5}}}{35}$		$-\frac{4\sqrt{\frac{3}{5}}}{35}$		
4	$M1E3\cdot M3E1$			$\frac{144}{49}$		$\frac{3}{49}$	
4	$M1E3\cdot E1M3$		$\frac{9}{7}$				
4	$M1E3\cdot E3M1$				$\frac{9}{7}$		
4	$M1E3\cdot E2M2$			$\frac{12\sqrt{\frac{3}{5}}}{7}$			
4	$M1E3\cdot E2E3$			$\frac{3\sqrt{15}}{7}$			
4	$M1E3\cdot E3E2$				$\frac{\sqrt{15}}{7}$		
4	$M2E2^2$	$\frac{36}{25}$		$\frac{36}{245}$		$\frac{16}{1225}$	
4	$M2E2\cdot M3E1$		$\frac{144\sqrt{\frac{3}{5}}}{35}$		$-\frac{4\sqrt{\frac{3}{5}}}{35}$		
4	$M2E2\cdot E1M3$			$\frac{12\sqrt{\frac{3}{5}}}{7}$			
4	$M2E2\cdot E2M2$		$\frac{24}{25}$		$\frac{72}{175}$		
4	$M2E2\cdot E3M1$			$\frac{12\sqrt{\frac{3}{5}}}{7}$			
4	$M2E2\cdot E2E3$		$\frac{48}{35}$		$\frac{12}{35}$		
4	$M2E2\cdot E3E2$			$\frac{36}{49}$		$-\frac{8}{49}$	
4	$M3E1^2$	$\frac{12}{7}$		$-\frac{3}{14}$			
4	$M3E1\cdot E1M3$				$\frac{9}{7}$		
4	$M3E1\cdot E2M2$			$\frac{12\sqrt{\frac{3}{5}}}{7}$			
4	$M3E1\cdot E3M1$		$\frac{9}{7}$				
4	$M3E1\cdot E2E3$			$\frac{24\sqrt{15}}{49}$		$-\frac{3\sqrt{15}}{49}$	
4	$M3E1\cdot E3E2$		$\frac{9\sqrt{\frac{3}{5}}}{7}$		$-\frac{4\sqrt{\frac{3}{5}}}{7}$		

Supplementary Table 3: The coefficients a_l^ξ of the Legendre polynomials in supplementary Eq. (13) for the case of an $11/2^-$ to $3/2^+$ transition. The symbol ξ stands for a full set of parameters $\{S_1'L_1'S_1L_1S_2'L_2'S_2L_2\}$. For instance, $M1E3^2$ means $S_1' = S_2' = 1$, $L_1' = L_2' = 1$, $S_1 = S_2 = 0$, $L_1 = L_2 = 3$. For not listed combinations of ξ the value of $a_l^\xi = 0$. All fully stretched $J = 4$, and $E2E3$ and $E3E2$ ($J = 4, 5$) were included. Continues in table 4.

J	$\xi = (S'_1L'_1S_1L_1)\cdot(S'_2L'_2S_2L_2)$	a_0^ξ	a_1^ξ	a_2^ξ	a_3^ξ	a_4^ξ	a_5^ξ
4	$E1M3^2$	$\frac{12}{7}$		$-\frac{3}{14}$			
4	$E1M3\cdot E2M2$		$\frac{144\sqrt{\frac{3}{5}}}{35}$		$-\frac{4\sqrt{\frac{3}{5}}}{35}$		
4	$E1M3\cdot E3M1$			$\frac{144}{49}$		$\frac{3}{49}$	
4	$E1M3\cdot E2E3$		$-\frac{9\sqrt{\frac{3}{5}}}{7}$		$\frac{4\sqrt{\frac{3}{5}}}{7}$		
4	$E1M3\cdot E3E2$			$-\frac{24\sqrt{15}}{49}$		$\frac{3\sqrt{15}}{49}$	
4	$E2M2^2$	$\frac{36}{25}$		$\frac{36}{245}$		$\frac{16}{1225}$	
4	$E2M2\cdot E3M1$		$\frac{144\sqrt{\frac{3}{5}}}{35}$		$-\frac{4\sqrt{\frac{3}{5}}}{35}$		
4	$E2M2\cdot E2E3$			$-\frac{36}{49}$		$\frac{8}{49}$	
4	$E2M2\cdot E3E2$		$-\frac{48}{35}$		$-\frac{12}{35}$		
4	$E3M1^2$	$\frac{12}{7}$		$-\frac{3}{14}$			
4	$E3M1\cdot E2E3$				$-\frac{\sqrt{15}}{7}$		
4	$E3M1\cdot E3E2$			$-\frac{3\sqrt{15}}{7}$			
4	$E2E3^2$	$\frac{36}{35}$		$-\frac{27}{98}$		$\frac{8}{245}$	
4	$E2E3\cdot E3E2$		$\frac{384}{245}$		$-\frac{1}{5}$		$-\frac{4}{49}$
4	$E3E2^2$	$\frac{36}{35}$		$-\frac{27}{98}$		$\frac{8}{245}$	
5	$E2E3^2$	$\frac{44}{35}$		$\frac{11}{49}$		$-\frac{4}{735}$	
5	$E2E3\cdot E3E2$		$\frac{704}{245}$		$\frac{22}{315}$		$\frac{4}{441}$
5	$E3E2^2$	$\frac{44}{35}$		$\frac{11}{49}$		$-\frac{4}{735}$	

Supplementary Table 4: Continued from supplementary table 3.